Low-spin electromagnetic transition probabilities in ^{102,104}Cd

N. Boelaert,* A. Dewald, C. Fransen, J. Jolie, A. Linnemann, B. Melon, and O. Möller
Institut für Kernphysik, Universität zu Köln, Zülpicher Straße 77, D-50937 Köln, Germany

N. Smirnova and K. Heyde
Department of Subatomic and Radiation Physics, Ghent University, Proeftuinstraat 86, B-9000 Gent, Belgium

(Dated: January 18, 2007)

Lifetimes of low-lying states in ^{102,104}Cd were determined by using the recoil distance Doppler-shift technique with a plunger device and a Ge array consisting of five HP Ge detectors and one Euroball cluster detector. The experiments were carried out at the Cologne FN Tandem facility using the ^{92}Mo(^{12}C,2n)^{102}Cd reaction at 41 MeV and the ^{94}Mo(^{12}C,2n)^{104}Cd reaction at 42 MeV. The Differential Decay Curve Method in coincidence mode was employed to derive the lifetime of the first 2^+ state in both nuclei and the lifetime of the 4^+ state in ^{104}Cd. The corresponding reduced E2 transition probabilities have been studied within the framework of the nuclear shell model.

PACS numbers: 21.10.Tg, 21.60.Cs, 27.60.+j

I. INTRODUCTION

Cadmium isotopes are of considerable interest due to the fact that they are only two proton holes away from the Z=50 shell. Over the last decades they have been intensively studied, notably in the context of multiphonon states of quadrupole [1–13] and of quadrupole-octupole nature [5, 6, 14–17]. Of special interest for the former is their interaction with intruding 2p-2h proton excitations across the Z=50 shell, leading to shape coexistence of spherical normal and deformed intruder states [18–21].

To extent our knowledge to the light Cadmium isotopes, ^{102}Cd and ^{104}Cd are particularly important because they lie in the transitional region which connects the nuclei showing single-particle behaviour, like ^{98}Cd [22] and those of collective behaviour, similar to the heavier vibrational-like Cd isotopes. Here the connection between collective and shell model descriptions can be made.

A lot of research on high-spin structure and electromagnetic transition strengths has been carried out in ^{102}Cd [23–25] and in ^{104}Cd [26, 27]. In this work, which focuses on low-spin states, we have measured the lifetimes of the first 2^+ and 4^+ states of the ground-state band in ^{104}Cd and of the first 2^+ state in ^{102}Cd by employing the recoil-distance Doppler-shift (RDDS) technique. The aim of our experiment was to investigate the collectivity of these nuclei from their B(E2) strength and to test whether shell-model calculations are able to reproduce the onset of collectivity.

The experiments are described in Sec. II. The analyses of the experiments on ^{104}Cd and ^{102}Cd is presented in Sec. III and IV, respectively. Sec. V presents the comparison of our results with shell-model calculations. Finally, the paper closes with the conclusions (Sec. VI).

*Also at the Department of Subatomic and Radiation Physics, Ghent University, Proeftuinstraat 86, B-9000 Gent, Belgium

II. PERFORMED EXPERIMENTS

A. RDDS technique

Two recoil distance Doppler-shift (RDDS) experiments have been performed with the Cologne coincidence plunger device at the FN Tandem facility at the University of Cologne in order to determine the lifetimes of low-lying excited states in ^{102,104}Cd.

The lifetimes were obtained using the Differential Decay Curve Method (DDCM) for $\gamma-\gamma$ coincidences [28]. This method avoids problems related to the feeding history of the state of interest, especially the problem of unobserved side feeding.

In the particular case of gating on the shifted component of a direct-feeding transition of state i, the lifetime of this state can be determined with the following formula [28]:

$$\tau(x) = \frac{I_u^{BA}(x)}{v.\frac{d}{dx}I_s^{BA}(x)}, \qquad (1)$$

where v denotes the recoil velocity and the quantities $I_u^{BA}(x)$ and $I_s^{BA}(x)$ stand for the normalized intensities of the respectively unshifted (u) and shifted (s) component of a depopulating transition A in coincidence with the shifted component of the populating transition B at the target-to-stopper distance x.

B. ^{104}Cd-experiment

Recently, lifetime measurements of ^{104}Cd using the Cologne plunger device were performed by Müller *et al.* [27]. They used the ^{58}Ni(^{50}Cr,4p) reaction at a beam energy of 205 MeV which populated high-spin states up

to spin of 20 $\hbar$. The lifetime of the 2_1^+ state has been determined with an error of 33% to be 9(3) ps. For the lifetime of the 4_1^+ state only an upper limit of 6 ps could be determined.

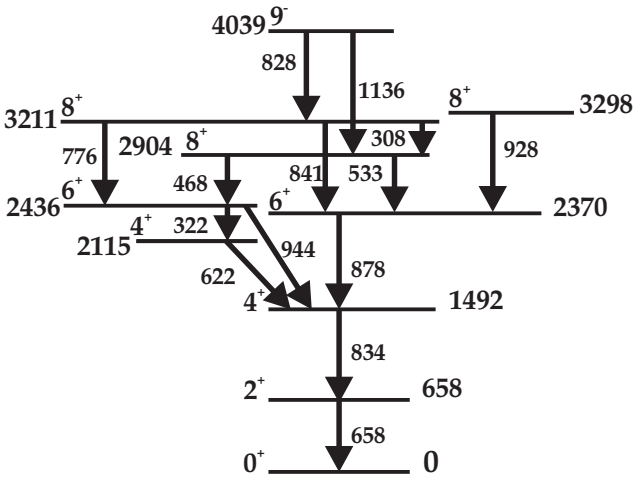

FIG. 1: Partial level Scheme of ^{104}Cd [27].

The main problem was the strong population of a long lived 8^+ state at 2904 keV with a lifetime of 1.23(7) ns. The relevant part of the level scheme of ^{104}Cd, taken from the work of Müller *et al.* [27], is presented in Fig. 1. In order to determine lifetimes of lower lying states, which are expected to be in the picosecond range, a dominant feeding of these states via the long-lived 8^+ state should be avoided. Therefore, we used the reaction ^{94}Mo(^{12}C,2n)^{104}Cd at an optimal beam energy of 42 MeV. The calculated cross section for this reaction was 80 mb and the maximum spin transfer was 12 $\hbar$ as estimated by the computer code CASCADE [29]. The target was a 0.5 mg/cm^2 selfsupporting foil of 99% enriched ^{94}Mo and the stopper was a 5 mg/cm^2 gold foil. The mean recoil velocity, derived from the energy shifts between the Doppler shifted and the unshifted components of nuclear transitions, was 0.747(2) $\times 10^{-2}$c, with c the velocity of light.

The experimental setup (Fig. 2) consisted of one Euroball cluster detector, made out of 7 encapsulated Ge-detectors, at 0° relative to the beam axis and five HP Ge detectors at a polar angle of 143°. The twelve large volume Ge detectors had an efficiency of about 55% each. The six outer segments of the cluster form a ring (assigned as ring 1 in the following) with a polar angle of 31° with respect to the beam axis. The five detectors in the backward direction form a second ring (ring 2). The central capsule of the cluster is positioned at an angle of 0° with the beam axis.

We have measured all eight possible coincidences between the two rings and the central detector, but because of the lack of sufficient statistics, coincidence spectra of the central detector were not used. Denoting gated spectra with A-B we considered the combinations 1-0, 1-1,

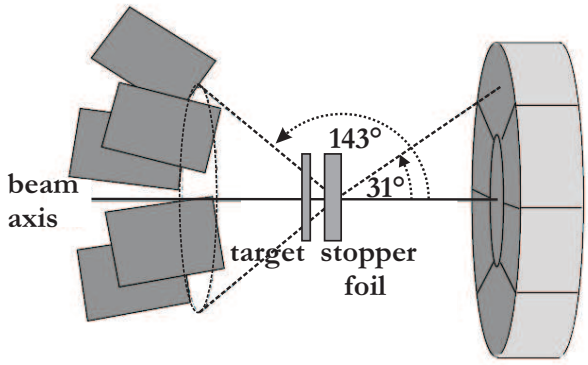

FIG. 2: Schematic drawing of the experimental setup.

1-2, 2-0, 2-1 and 2-2. In this shorthand notation B is the ring we gate on and A is the ring we look on. 0 stands for the central detector, 1 and 2 stand for ring 1 and ring 2 respectively.

With our setup and by using eq. 1 we were able to determine lifetimes in a forward angle (ring 1) and in a backward angle (ring 2) by gating on as many rings as possible. In this way two independent lifetimes were derived and used to check their consistency.

We have measured two sets of distances; set A with ten distances and set B with twelve distance. Those sets have not been combined because of different unknown off-sets in the distance calibrations. All relative distances were between 1 and 300 μm.

The normalized intensities which enter into eq. 1 at each target-to-stopper distance x were determined by using the corresponding peaks in the gated spectra and normalising them to the total number of excited Cd nuclei produced at that distance. In practice this normalization has been done by gating on the shifted and the unshifted component of the $2_1^+ \rightarrow 0_1^+$ transition for each distance and determining the intensities of the shifted and unshifted components of higher transitions, more specifically of the $4_1^+ \rightarrow 2_1^+$ and the $6_1^+ \rightarrow 4_1^+$ transitions. The sum of the shifted and unshifted component of a higher transition is proportional to the total number of produced nuclei and because this proportionality is the same for each distance, this allows a normalization. Using two higher transitions in gated spectra both in ring 1 and in ring 2 we determined 4 sets of normalization coefficients and checked the consistency. We also checked for the need to correct the coincidence matrix for deorientation effects by taking the intensity ratios $I_{u+s}^{4\rightarrow 2,2\rightarrow 0}(x)/I_{u+s}^{4\rightarrow 2,6\rightarrow 4}(x)$. The deorientation, which affects mostly the $2_1^+ \rightarrow 0_1^+$ transition would show a change of this ratio for longer distances towards smaller values. We did not observe such a change within our experimental accuracy. Note that the detectors used are not positioned at optimal angles for observing a deorientation effect. We could only show that the data which enter into the actual lifetime analysis needs no correction for

the deorientation effect.

The derivative in eq. 1, $\frac{d}{dx} I_s^{BA}(x)$, was calculated by fitting piecewise continuously differentiable second-order polynomials to the intensity values $I_u^{BA}(x)$ using the computer code NAPATAU [30]. Since the lifetimes τ are calculated for every distance x one obtains a function $\tau(x)$ or $\tau(t)$ with $t = x/v$; i.e. the so-called τ-curve which is expected to be a constant. Deviations from a constant behavior indicate the presence of systematic errors. The adopted lifetime is obtained by averaging the $\tau(x)$-values within the so-called region of sensitivity [28, 30]. Outside this region the statistical errors become too large.

C. ^{102}Cd-experiment

Fig. 3 shows the relevant part of the most comprehensive level scheme of ^{102}Cd taken from the work of Lieb *et al.* [25]. They used the ^{58}Ni(^{50}Cr,α 2p) reaction at a beam energy of 205 MeV. Using the Cologne plunger device several lifetimes have been determined by using the DDCM technique, but for the lowest 2^+ and 4^+ states only upper limits of 8.1 ps have been obtained.

The isomeric 8_1^+ state appears at an energy of 2718 keV and has a lifetime of 56(4) ns. This is the longest lifetime in ^{102}Cd that has been determined so far. To determine lifetimes of states below this 8^+ state, this state should not be strongly populated in the fusion reaction.

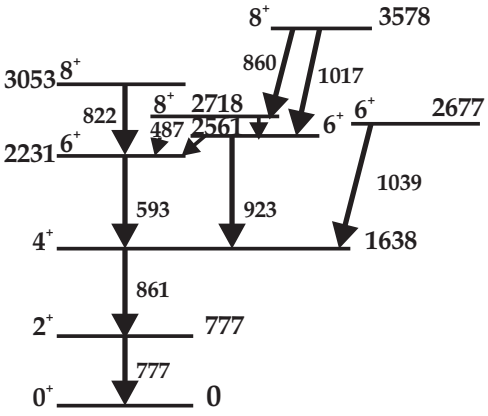

FIG. 3: Partial level scheme of ^{102}Cd taken from the work of Lieb *et al.* [25].

Therefore, we have used the ^{92}Mo(^{12}C,2n)^{102}Cd fusion evaporation reaction at a beam energy of 41 MeV to populate excited states in ^{102}Cd. A calculation with the computer code CASCADE [29] predicts a calculated cross section in the (2n)-channel of 27 mb and a maximum spin transfer of $9\hbar$. The target was a 1mg/cm^2 selfsupporting foil of 99% enriched ^{92}Mo and the stopper was a 5mg/cm^2 gold foil. The mean recoil velocity was $0.726(6) \times 10^{-2}$c.

The setup for this experiment was the same as in the case of the ^{104}Cd experiment (see Sec. II B). Only one set with eight different target-to-stopper distances between 2 and 100 μm has been used.

III. EXPERIMENTAL RESULTS FOR ^{104}Cd.

In Figure 4 some gated spectra for data set A are shown for the $2_1^+ \rightarrow 0_1^+$ and $4_1^+ \rightarrow 2_1^+$ transitions measured at three different distances. The gate is set on the shifted component of the $6_1^+ \rightarrow 4_1^+$ transition. Despite the fact that the 6_1^+ is characterised by a relative high excitation energy (2.4 MeV) the spectra exhibit good statistics.

A. Lifetime of the 2_1^+ state

To determine the lifetime of the 2_1^+ state at an excitation energy of 658 keV, we have placed a gate on the Doppler shifted component of the $4_1^+ \rightarrow 2_1^+$ transition at an energy of 834.1 keV (see Fig. 1).

Unfortunately, the Doppler shifted component of this transition overlaps in the centre segment and in ring 1 (the forward ring) with the unshifted component of the $8_3^+ \rightarrow 6_1^+$ transition at energy 841.2 keV and for ring 2 (the backward ring) with the unshifted component of the $9_1^- \rightarrow 8_3^+$ transition at energy 828.3 keV.

This overlap has caused extra unshifted intensity in lower transitions, such as the $2_1^+ \rightarrow 0_1^+$ transition. This extra amount of intensity was unwanted because it has prevented the determination of $I_u^{BA}(x)$ in eq. 1 from the gated spectra. But because the extra amount – after correction for the energy efficiency – is the same for the transitions $6_1^+ \rightarrow 4_1^+$, $4_1^+ \rightarrow 2_1^+$ and $2_1^+ \rightarrow 0_1^+$ we were able to determine in the gated spectra this extra amount in the $2_1^+ \rightarrow 0_1^+$ transition from the unshifted intensity of the $6_1^+ \rightarrow 4_1^+$ transition and subtract it from the unshifted intensity of the $2_1^+ \rightarrow 0_1^+$ transition.

Following this method we have determined the lifetime from the spectra in ring 1 and ring 2 for the two data sets (Tab. I). As is clear from the values we have obtained consistent results yielding a weighted average for the lifetime of 8.5 ± 0.3 ps. This value agrees with the previous measurement [27] but is an order of magnitude more precise.

τ [ps]	ring 1	ring 2
set A	8.4 ± 0.8	8.2 ± 0.5
set B	8.7 ± 0.5	8.8 ± 0.6

TABLE I: Experimentally determined values for the lifetime of the 2_1^+ state in ^{104}Cd using two data sets for target to stopper distances, for ring 1 and ring 2.

Fig. 5 shows the curves of the shifted and the unshifted intensities of the depopulating transition together with the τ-curve for ring 1 of set A. Within the sensitive region, indicated by dashed lines, constant lifetime values

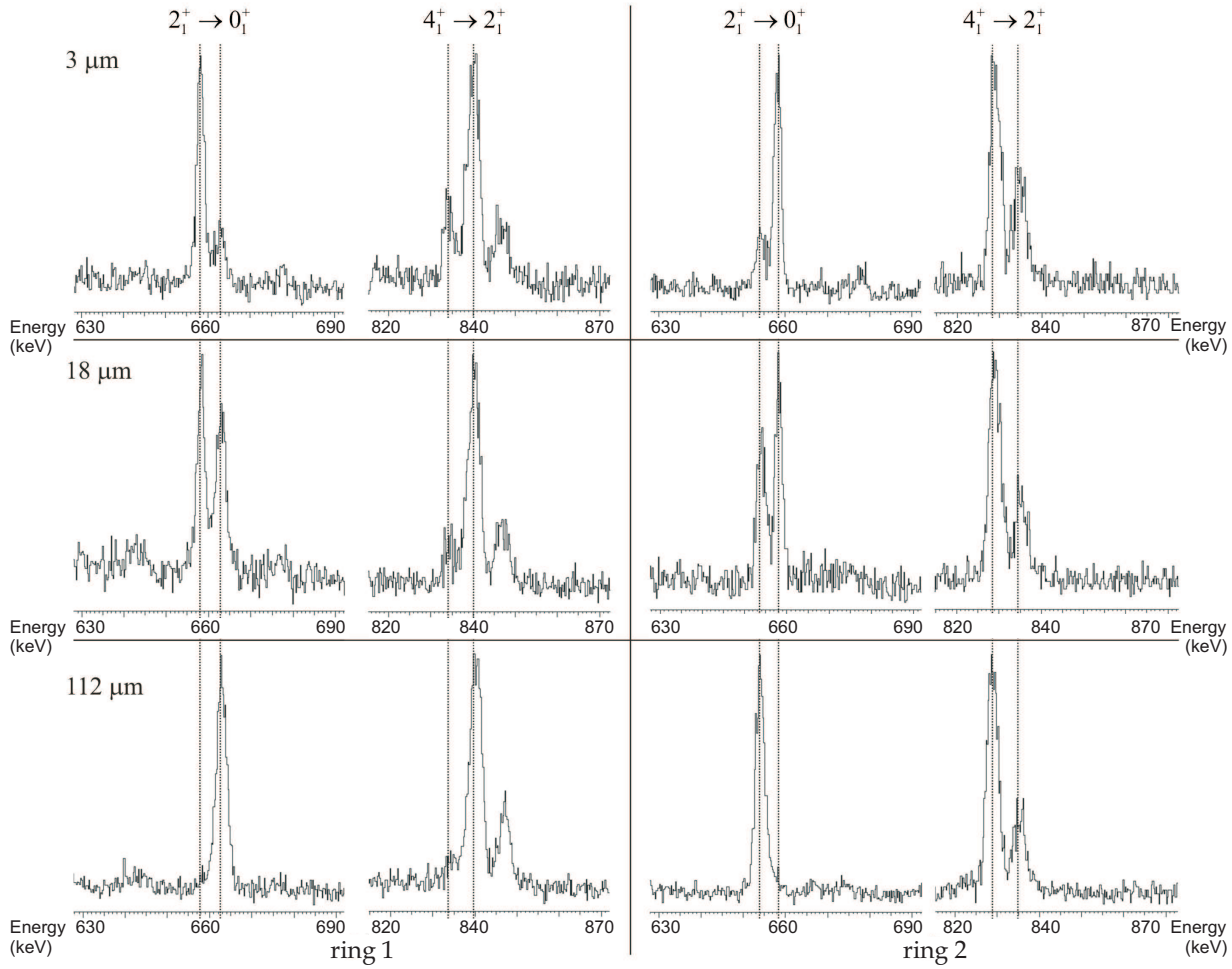

FIG. 4: Gated spectra with $2_1^+ \to 0_1^+$ and $4_1^+ \to 2_1^+$ transitions for three different distances. The gate is set on the Doppler shifted component of the $6_1^+ \to 4_1^+$ transition.

$\tau(x)$ were obtained.

B. Lifetime of the 4_1^+ state

We have placed a gate on the Doppler shifted component of the 878 keV transition (see Fig. 1). Notice that the unshifted component of the $4_1^+ \to 2_1^+$ transition is in overlap with the shifted component of the $8_3^+ \to 6_1^+$ transition at 841 keV in the backward ring and with the shifted component of the $9_1^- \to 8_3^+$ transition at 828 keV in the forward rings, so that a correct analysis becomes impossible if the lifetimes of the 9_1^- or the 8_3^+ are equal or shorter than the lifetime of interest.

By gating on the 834 keV transition and using the backward ring spectra we were able to prove that the lifetime of the 9_1^- is long enough to not affect our results, because we did not observe shifted components of the $9_1^- \to 8_3^+$ transition. At forward angle we observed a shifted component indicating that the lifetime of the 8_3^+ is too short, so that we could only determine the lifetime of the 4_1^+ using spectra of ring 1. Because the distances in set A were not suited for a short lifetime, we used only data from set B and obtained the value 1.5 ± 0.5 ps. Fig. 5 shows the curves of the shifted and the unshifted intensities of the depopulating transition together with the τ-curve.

IV. EXPERIMENTAL RESULTS FOR ^{102}Cd

In this experiment only the lifetime of the first 2^+ state has been determined because there was not enough statistics to determine the lifetime of higher states. Fig. 6 shows for three different distances the $2_1^+ \to 0_1^+$ transition gated by the shifted component of the $4_1^+ \to 2_1^+$ transition.

The lifetime of the 2_1^+ state was determined using only data from ring 2 by gating on the shifted component of the populating transition $4_1^+ \to 2_1^+$. We obtained a lifetime of 5.1±0.8 ps. Fig. 7 shows the curves with unshifted and shifted intensities of the depopulating transition and

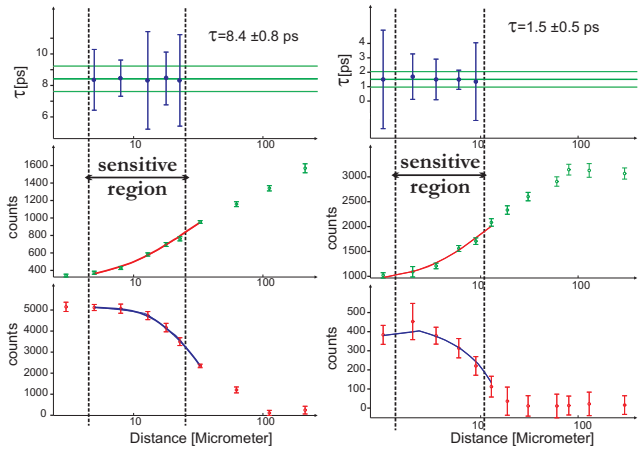

FIG. 5: (Color online) Analysis of the lifetime of the 2_1^+ state for set A (left) and of the 4_1^+ state for set B (right), both for ring 1: curves with unshifted (bottom) and shifted (middle) intensities of the depopulating transitions and τ-curves (top).

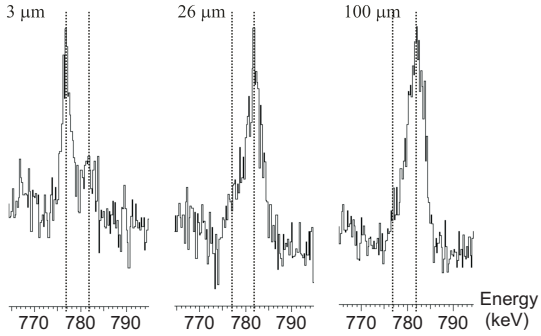

FIG. 6: The $2_1^+ \rightarrow 0_1^+$ transition gated by the shifted component of the $4_1^+ \rightarrow 2_1^+$ transition for three different distances.

the τ-curve.

V. COMPARISON WITH SHELL-MODEL CALCULATIONS

Shell-model calculations have been performed using the code ANTOINE [31]. The low-lying energy spectra and E2 transition probabilities of the Cd isotopes with neutron numbers from N=50 to N=56 have been calculated using the core $^{88}_{38}\mathrm{Sr}_{50}$ together with the $\{2p_{1/2}, 1g_{9/2}\}$ proton valence space and the $\{2d_{5/2}, 3s_{1/2}, 2d_{3/2}, 1g_{7/2}, 1h_{11/2}\}$ neutron valence space. The single-particle energies are taken from [32]. We have used the effective realistic interaction constructed by Smirnova *et al.* [33]. B(E2)-values of low-lying states have been calculated with the effective charges e_π=1.7e and e_ν=1.1e. More details including the results for $^{100-106}$Cd will be presented in an upcoming article [34].

Besides a more detailed discussion of the particular energy spectra and electromagnetic E2 decay properties in ^{102,104}Cd, we also address the issue of how collectivity can develop studying the energy spectra and B(E2) reduced transtion probabilities starting at the N=50 neutron closed shell and moving onwards to N=58 in ^{106}Cd.

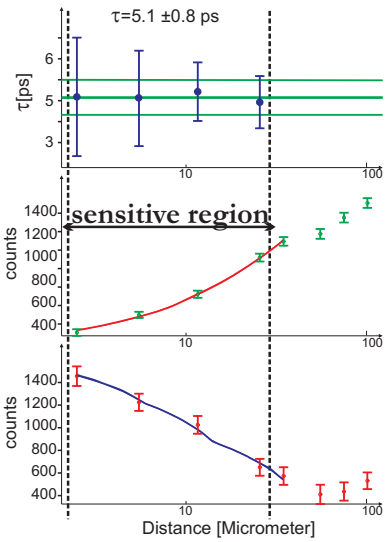

FIG. 7: (Color online) Analysis of the lifetime of the 2_1^+ state for ring 2: curves with unshifted and shifted intensity of the depopulating transition and τ-curve.

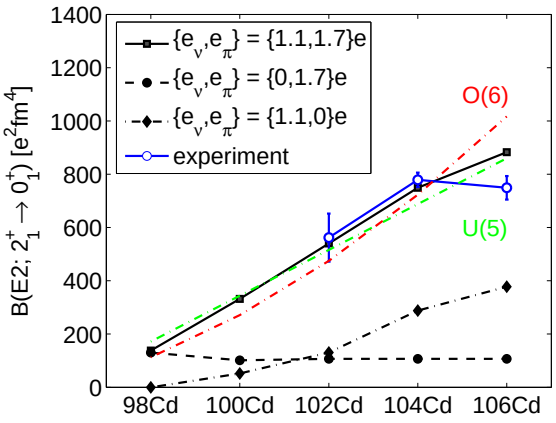

FIG. 8: (Color online) Experimental, Shell-model (with $\{e_\pi, e_\nu\}$ =$\{1.7, 1.1\}$, $\{0.0, 1.1\}$ and $\{1.7, 0.0\}$) and collective (U(5) and O(6)) $B(E2; 2_1^+ \rightarrow 0_1^+)$ values for the different Cd nuclei.

In figs. 8 to 11, we present the particularly important B(E2) reduced transtion probabilities for the $2_1^+ \rightarrow 0_1^+$, $4_1^+ \rightarrow 2_1^+$, $6_1^+ \rightarrow 4_1^+$ and $8_i^+ \rightarrow 6_1^+$ (from the lowest collective 8^+ level), In each of those cases we give the separate proton and neutron contributions that are always adding up coherently. It is remarkable to note that for the $2_1^+ \rightarrow 0_1^+$ E2 transition, the shell-model results follow the trend in the available data rather well. Moreover, the B(E2) value increases almost linearly with the number of neutron pairs which is precisely the dependence that

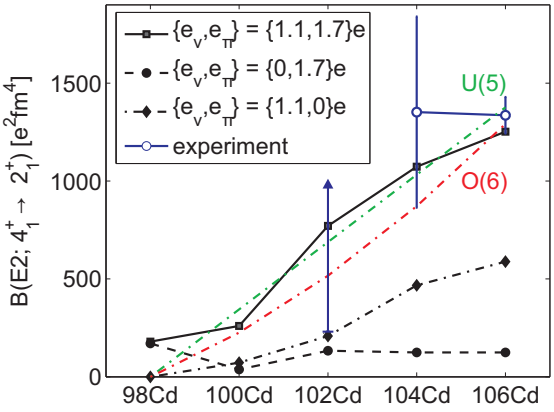

FIG. 9: (Color online) Experimental, Shell-model (with $\{e_\pi, e_\nu\}$ ={1.7, 1.1}, {0.0, 1.1} and {1.7, 0.0}) and collective (U(5) and O(6)) $B(E2; 4_1^+ \rightarrow 2_1^+)$ values for the different Cd nuclei.

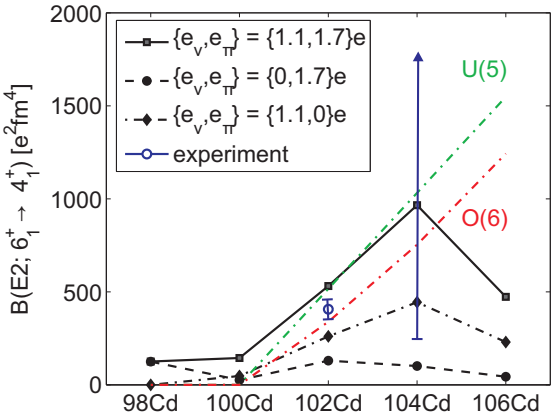

FIG. 10: (Color online) Experimental, Shell-model (with $\{e_\pi, e_\nu\}$ ={1.7, 1.1}, {0.0, 1.1} and {1.7, 0.0}) and collective (U(5) and O(6)) $B(E2; 6_1^+ \rightarrow 4_1^+)$ values for the different Cd nuclei.

results from both a collective U(5) and O(6) symmetry [35]. These results give an interesting view on the possibilities to develop the collective structure originating from the increasing importance of the neutron contribution with almost constant proton contribution as can be seen in fig. 8. In view of the deviation in the case of ^{106}Cd, a remeasurement of the experimental value would be very useful. For the $4_1^+ \rightarrow 2_1^+$ E2 transition (see fig. 9), the increase exhibited in the shell-model results first remains about constant but then increases again almost linearly with the number of neutrons, flattening somewhat towards ^{106}Cd. The structure resembles the U(5) and O(6) behavior rather well, starting from ^{100}Cd, since this is the first nucleus in which a collective 4^+ could appear counting nucleon pairs from Z=50, N=50. For both the $6_1^+ \rightarrow 4_1^+$ and the collective $8_i^+ \rightarrow 6_1^+$ E2 transtions

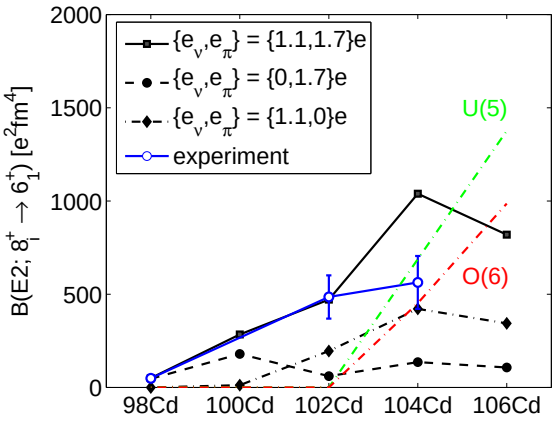

FIG. 11: (Color online) Experimental, Shell-model (with $\{e_\pi, e_\nu\}$ ={1.7, 1.1}, {0.0, 1.1} and {1.7, 0.0}) and collective (U(5) and O(6)) $B(E2; 8_i^+ \rightarrow 6_1^+)$ values for the different Cd nuclei, with $i = 1$ for ^{98,100}Cd, $i = 2$ for ^{102}Cd and $i = 3$ for ^{104,106}Cd.

(figs. 10 and 11), there are not that many data to compare with but the retarded increase for the lighter Cd nuclei and the increase towards ^{104}Cd, which is quite linear, do show up in the shell-model results. The drop in moving towards ^{106}Cd is most possibly related to the truncation that was used in the latter nucleus, as can be seen in the drop of the neutron E2 contribution in figs. 10 and 11. A general outcome, however, is the clear built-up of collectivity with increasing neutron number and this in a way that shows a smooth increase which approximately scales with the number of neutron pairs outside of N=50.

We now discuss more in particular the detailed spectroscopic data and the shell-model results obtained in the present study for ^{102,104}Cd. The overall agreement in the energy spectra, as depicted in fig. 12, is very good and this comparison is supported when comparing the experimentally extracted B(E2) values with the shell-model calculations (see Tab. II for details). Inspecting the energy spectra, one notices that once beyond the 4^+ state, there are various $6^+, 8^+$ and 10^+ states. So there it is important to carry out a careful study of the B(E2) values in order to see if there is a more collective state that stands out for each of these spin values and how they compare with the data. The energy spectra, even approaching ^{104,106}Cd, are clearly more complex than purely collective models, invoking vibrational or gamma-soft structures, indicate. This particular interplay between collective and less collective structures can therefore be acommodated through the nuclear shell model.

In the case of ^{102}Cd, the lowest 2^+ and 4^+ can rather well be associated with collective states and this is supported when comparing the corresponding B(E2) values as given in Tab. II. In the E2 decay from the next two 6^+ states, it is unambigous that the 6_1^+ level carries the collective decay as also shown in Tab. II. In moving upwards in order to construct a collective sequence, we have

	E_{level} [keV]	J_i^π	τ [ps]	E_γ [keV]	J_f^π	$B(E2)_{exp}$ $[e^2fm^4]$	$B(E2)_{calc}$ $[e^2fm^4]$	U(5) $[e^2fm^4]$	O(6) $[e^2fm^4]$
^{102}Cd	777	2_1^+	5.9(5)	777	0_1^+	562(90)^a	540	562	562
	1638	4_1^+	<8.1	861	2_1^+	>225^b	771	749	611
	2231	6_1^+	28(2)	593	4^+	406(27)^b	531	562	401
	2718	8_1^+	56(4)ns	487	6_1^+	0.17(2)^b	51		
	3053	8_2^+	4.5(10)	822	6_1^+	485(116)^b	471		
^{104}Cd	658	2_1^+	8.5(12)	658	0_1^+	779(27)^a	749	779	779
	1492	4_1^+	1.5(5)	834	2_1^+	1352(488)^a	1073	1168	937
	2370	6_1^+	<6	878	4_1^+	>246^c	966	1168	937
	2436	6_2^+	84(20)	322	4_2^+	$595(^{60}_{50})^c$	325		
				944	4_1^+	10.3(8)^c	17		
	2904	8_1^+	1.23(7)ns	468	6_2^+	1.4(2)^c	2.6		
				533	6_1^+	14.7(8)^c	1.6		
	3211	8_2^+	<7	776	6_2^+	>161^c	41		
				841	6_1^+	>134^c	41		
	3298	8_3^+	1.5(3)	863	6_2^+	$329(^{58}_{85})^c$	708		
				928	6_1^+	$563(^{142}_{95})^c$	1039	779	486

[a]From this work.
[b]From Ref. [25].
[c]From Ref. [27].

TABLE II: Experimental, shell-model ($\{\tilde{e}_\nu, \tilde{e}_\pi\} = \{1.1, 1.7\}e$) and collective (U(5) and O(6)) BE(2) values.

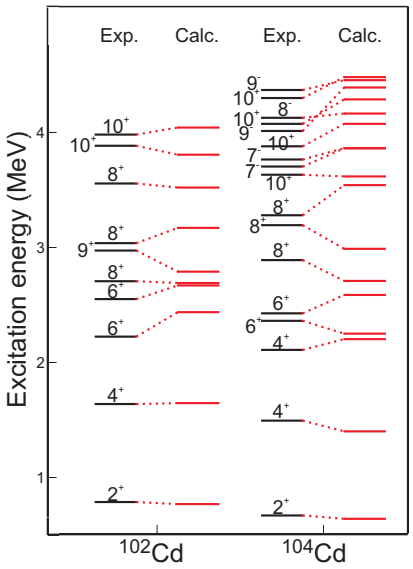

FIG. 12: (Color online) Experimental and theoretical energy spectra of ^{102,104}Cd.

calculated the E2 decay originating from the various 8^+ states. From Tab. II it becomes clear that the collective path selects the 8_2^+ level by a factor 10 in reduced transition probability over the decay from the 8_1^+ level, Experimentally, the weak $8_1^+ \rightarrow 6_1^+$ B(E2) value of 0.17(2) $e^2.fm^4$ is much smaller than the theoretical value of 51 $e^2.fm^4$. Even though there is a drop by a factor of 10 compared with the typically strongly collective E2 decay transition probabilities, we are not able to produce such a small value. Inspecting the relative proton and neutron contributions to that transition, the neutron contribution has dropped by almost a factor of 20 with respect to the collective case, the proton contribution remaining rather stable and both results are still in phase. Thus, the shell-model is still missing finer details when it comes to describing the very weak E2 transition rates. For this particular nucleus, there appears a rather distinct collective path starting from the ground state through the E2 sequence $0_1^+ \rightarrow 2_1^+ \rightarrow 4_1^+ \rightarrow 6_1^+ \rightarrow 8_2^+$. In Tab. II, we also compare with the yrast B(E2) reduced transition probabilties for both the U(5) and O(6) limits, normalizing to the experimental $B(E2; 2_1^+ \rightarrow 0_1^+)$ value. Due to the boson number restriction of N=3 we can only move up to the 6^+ E2 decay in ^{102}Cd. It appears that the U(5) numbers, to be taken as a guide only in this case, match relatively well both the experimental data and the shell-model results as far as the spin dependence in the band concerns.

For ^{104}Cd, the lowest 2^+ and 4^+ can again be associated with collective structures. Moreover, the shell model reproduces particularly well the experimental values, taking the rather large error bars into account. There now appear three 6^+ levels and two 4^+ states and the $B(E2; 6_1^+ \rightarrow 4_1^+)$ prolonges the collective path upwards, again consistent with the experimental value, although here only a lower limit is known. It is interesting to note that the 6_2^+ level also exhibits a strong E2 decay into the 4_2^+ level with an observable E2 branch into the 4_1^+ level, quite strongly in line with our present shell-model analysis. Thus, the structure is becoming much richer than would be expected from a vibrational model analysis. In moving to the higher-spin 8^+ states next, we notice that conform with the experimental weak B(E2) values associated with the decay from the 8_1^+ level to

the lower-lying $6^+_{1,2}$ levels, we obtain very weak values of 1.6 and 2.6 $e^2.fm^4$, respectively. There exist, however, only a lower limit of 134 $e^2.fm^4$ for the $B(E2;8^+_2 \rightarrow 6^+_1)$ value [27] and the $B(E2;8^+_3 \rightarrow 6^+_1)$ value amounts to $563(^{142}_{95})$ $e^2.fm^4$ [27]. The shell-model calculations result in a particularly strong $B(E2;8^+_3 \rightarrow 6^+_1)$ value of 1039 $e^2.fm^4$ whereas the $B(E2;8^+_2 \rightarrow 6^+_1)$ value is 41 $e^2.fm^4$. This points most possibly towards a collective $8^+_3 \rightarrow 6^+_1$ E2 transition, however, the fragmentation on the experimental side is more pronounced. In table II, we give all possible $8^+_i \rightarrow 6^+_k$ theoretical B(E2) values (with $i = 1, 2, 3$ and $k = 1, 2$) resulting from the present calculations. So, the shell-model is indicating a rather good agreement with all available B(E2) values, indicating the fact the effective interaction used at present is able to create the necessary correlations that result in both a collective path i.e. the $0^+_1 \rightarrow 2^+_1 \rightarrow 4^+_1 \rightarrow 6^+_1 \rightarrow 8^+_3$ sequence, as well as a number of less collective states. As in the case of ^{102}Cd, we compare with the predictions of a pure U(5) and O(6) in which the spin dependence is given in Tab. II.

VI. CONCLUSIONS

Two lifetimes in ^{104}Cd and one lifetime in ^{102}Cd have been measured by using the recoil distance Doppler shift technique with the Differential Decay Curve Method in the coincidence mode. In order to avoid a strong population of isomeric 8^+ states, reactions slightly above the Coulomb barrier were used. This leads to a moderate angular momentum transfer at the price of low cross sections.

The experimental results have been compared with shell-model calculations that make use of the code ANTOINE. In these calculations, we consider as the core nucleus ^{88}Sr and the full valence space of available protons between 38 and 50, i.e. the $2p_{1/2}$ and $1g_{9/2}$ orbitals, and of available neutrons between 50 and 82, i.e. the $2d_{5/2}$, $1g_{7/2}$, $2d_{3/2}$, $3s_{1/2}$ and $1h_{11/2}$ orbitals are considered. We carefully study the reduced E2 transition probabilities for the Cd nuclei spanning the region N=50 up to N=58 in order to explore the way in which collective structures develop when the neutron number is increasing. More in particular the $2^+_1 \rightarrow 0^+_1$, $4^+_1 \rightarrow 2^+_1$, $6^+_1 \rightarrow 4^+_1$ and $8^+_i \rightarrow 6^+_1$ (from the lowest collective 8^+ level) B(E2) values are presented, The energy spectra and B(E2) reduced transition probabilities in ^{102,104}Cd are generally well described by the shell-model calculations as carried out in the present paper. In each of these nuclei, we can identify a collective sequence of E2 transtions $0^+_1 \rightarrow 2^+_1 \rightarrow 4^+_1 \rightarrow 6^+_1 \rightarrow 8^+_i$ with i=2 for ^{102}Cd and i=3 in the case of ^{104}Cd pointing towards coherence between the proton and neutron contributions establishing a clear signature of collective effects. Details are presented in table II in which we also compare the B(E2) values with purely collective models such as the U(5) and O(6) limits of the interacting boson model. The results obtained in the present study indicate evidence for richer structures in which both collective and less collective states can develop within a shell-model scheme. The results also shed new light on the way in which collective effects gradually built up from the underlying proton and neutron contributions and the associated coherence.

Acknowledgments

N.S. thanks E. Caurier and F. Nowacki for making available their ANTOINE shell-model code and many fruitful discussions. This work was supported by the Deutsche Forschungsgemeinschaft under grant JO 391/3-2 and by the interuniversity Attraction Pool (IUAP) under project P5/07. K.H. is grateful to the FWO-Vlaanderen for financial support.

[1] A. Aprahamian, D. S. Brenner, R. F. Casten, R. L. Gill, A. Piotrowski, and K. Heyde, Phys. Lett. **140B**, 22 (1984).
[2] A. Aprahamian, D. S. Brenner, R. F. Casten, R. L. Gill, and A. Piotrowski, Phys. Rev. Lett. **59**, 535 (1987).
[3] C. Fahlander, A. Bäcklin, L. Hasselgren, A. Kavka, V. Mittal, L. E. Svensson, B. Varnestig, D. Cline, B. Kotlinski, H. Grein, E. Grosse, R. Kulessa, C. Michel, W. Spreng, H. J. Wollersheim, J. Stachel, Nucl. Phys. **A485**, 327 (1988).
[4] M. Délèze, S. Drissi, J. Kern, P. A. Tercier, J. P. Vorlet, J. Rikovska, T. Otsuka, S. Judge, A. Williams, Nucl. Phys. **A551**, 269 (1993).
[5] M. Délèze, S. Drissi, J. Jolie, J. Kern, and J. P. Vorlet, Nucl. Phys. **A554**, 1 (1993).
[6] A. Gade, J. Jolie, and P. von Brentano, Phys. Rev. C **65**, 041305(R) (2002).
[7] M. Kadi, N. Warr, P. E. Garrett, J. Jolie and S. W. Yates, Phys. Rev. C **68**, 031306(R) (2003).
[8] R. F. Casten, J. Jolie, H. G. Börner, D. S. Brenner, N. V. Zamfir, W.-T. Chou, and A. Aprahamian. Phys. Lett. **B 297**, 19 (1992).
[9] F. Corminboeuf, T. B. Brown, L. Genilloud, C. D. Hannant, J. Jolie, J. Kern, N. Warr, and S. W. Yates, Phys. Rev. Lett. **84**, 4060 (2000).
[10] F. Corminboeuf, T. B. Brown, L. Genilloud, C. D. Hannant, J. Jolie, J. Kern, N. Warr, and S. W. Yates, Phys. Rev. C **63**, 014305 (2001).
[11] H. Lehmann, P. E. Garrett, J. Jolie, C. A. McGrath, Minfang Yeh, S. W. Yates, Phys. Lett. **B 387**, 259 (1996).
[12] A. Gade, A. Fitzler, C. Fransen, J. Jolie, S. Kasemann, H. Klein, A. Linnemann, V. Werner, and P. von Brentano, Phys. Rev. C **66** 034311 (2002).
[13] P. E. Garrett, H. Lehmann, J. Jolie, C. A. McGrath, Minfang Yeh, W. Younes, and S. W. Yates, Phys. Rev. C **64** 024316 (2001).

[14] D. Bandyopadhyay, C. C. Reynolds, S.R. Lesher, C. Fransen, N. Boukharouba, M.T. McEllistrem, and S. W. Yates, Phys. Rev. C **68**, 014324 (2003).
[15] S. E. Drissi, P. A. Tercier, H. G. Börner, M. Délèze, F. Hoyler, S. Judge, J. Kern, S. J. Mannanal, G. Mouze, K. Schreckenbach, J. P. Vorlet, N. Warr, A. Williams, C. Ythier, Nucl. Phys. **A614**, 137 (1997).
[16] P. E. Garrett, H. Lehmann, J. Jolie, C. A. McGrath, Minfang Yeh, and S. W. Yates, Phys. Rev. C **59**, 2455 (1999).
[17] A. Gade and P. von Brentano, Phys. Rev. C **66**, 014304 (2002).
[18] K. Heyde, P. Van Isaker, M. Waroquier and G. Wenes, Phys. Ref. **C25**, 3160 (1982).
[19] J. Kern, A. Bruder, S. Drissi, V. A. Ionescu, and D. Kusnezov, Nucl. Phys. **A512**, 1 (1990).
[20] J. Jolie and H. Lehmann, Phys. Lett. **B 342**, 19 (1995).
[21] H. Lehmann and J. Jolie, Nucl. Phys. **A 588**, 19 (1995).
[22] A. Blazhev *et al.*, Phys. Rev. C **69**, 064304 (2004).
[23] J. Tréherne, J. Genevey, A. Gizon, J. Gizon, R. Béraud, A. Chavret, R. Duffait, A. Emsallem, and M. Meyer, Zeit. f. Phys. A **309**, 135 (1982)
[24] J. Persson,*et al.* Nucl. Phys. A **627** 101 (1997).
[25] K. P. Lieb, D. Kast, A. Jungclaus, I.P. Johnstone, G. de Angelis, C. Fahlander, M. de Poli, P.G. Bizzeti, A. Dewald, R. Peusquens, H. Tiesler, M. Górska, and H. Grawe, Phys. Rev C **63** 054304 (2001).
[26] G. de Angelis,*et al.* Phys. Rev C **60** 014313 (1999).
[27] G. Müller,*et al.* Phys. Rev C **64** 014305 (2001).
[28] A. Dewald, S. Harissopulos, and P. von Brentano, Zeit. f. Phys. A **334**, 163 (1989).
[29] F. Pühlhofer, Nucl. Phys. A **280** 267 (1977).
[30] G. Böhm, A. Dewald, P. Petkov, and P. von Brentano, Nucl. Instr. & Meth. in Phys. Res.,**A329** 248 (1993).
[31] E. Caurier, E. and F. Nowacki, Acta Physica Polonica B **30**, 705 (1999).
[32] A. Holt, T. Engeland, M. Hjorth-Jensen, and E. Osnes, Phys. Rev C **61** 064318 (2000).
[33] N. Smirnova, et al., to be publ.
[34] N. Boelaert, N. Smirnova, K.L.G. Heyde, and J. Jolie, acc. for publ. in Phys. Rev. C.
[35] F. Iachello, and A. Arima, *The Interacting Boson Model,* Cambridge University Press, (1987).